Climate Dynamics manuscript No.
(will be inserted by the editor)

Future Trends of Snowfall Days in Northern Spain from ENSEMBLES Regional Climate Projections

M.R. Pons · S. Herrera · J.M. Gutiérrez

Received: date / Accepted: date

Abstract In a previous study Pons et al. (2010) reported a significant decreasing trend of snowfall occurrence in the Northern Iberian Peninsula since the mid seventies. The study was based on observations of annual snowfall frequency (measured as the annual Number of Snowfall Days NSD) from a network of 33 stations ranging from 60 to 1350 meters. In the present work we analyze the skill of Regional Climate Models (RCMs) to reproduce this trend for the period 1961-2000 (using both reanalysis– and historical GCM–driven boundary conditions) and the trend and the associated uncertainty of the regional future projections obtained under the A1B scenario for the first half of the 21st century. In particular, we consider the regional simulation dataset from the EU-funded ENSEMBLES project, consisting of thirteen state-of-the-art RCMs run at 25km resolution over Europe.

While ERA40 severely underestimates both the mean NSD and its observed trend (-2.2 days/ decade), the corresponding RCM simulations driven by the reanalysis appropriately capture the interannual variability and trends of the observed NSD (trends ranging from -3.4 to -0.7 days/decade, -2.1 days/decade for the ensemble mean). The results driven by the GCM historical runs are quite variable, with trends ranging from -8.5 to 0.2 days/decade (-1.5 days/decade for the ensemble mean), and the greatest uncertainty by far being associated with the particular GCM used. Finally, the trends for the future 2011–2050 A1B runs are more consistent and significant, ranging in this case from -3.7 to -0.5 days/decade (-2.0 days/decade for the ensemble mean), indicating a future significant decreasing trend. These trends are mainly determined by the increasing temperatures, as indicated by the interannual correlation between temperature and NSD (-0.63 in the observations), which is preserved in both ERA40– and GCM–driven simulations.

M.R. Pons
Agencia Estatal de Meteorología (AEMET), Santander, Spain
E-mail: mponsr@aemet.es

S. Herrera
Grupo de Meteorología. Dpto. de Matemática Aplicada y C.C. Universidad de Cantabria. Santander, Spain
E-mail: herreras@unican.es

J.M. Gutiérrez
Grupo de Meteorología. Instituto de Física de Cantabria (UC-CSIC), Santander, Spain E-mail: gutierjm@unican.es

Keywords ENSEMBLES · dynamical downscaling · regional climate modeling · snowfall occurrence · snowfall trends · climate change

1 Introduction

The analysis of climate trends has become an important research topic during the last decades. As a result many global and regional trend studies are nowadays available, mostly for temperature and precipitation (see, e.g. Trenberth et al., 2007). However, other variables of interest —such as snow— have received less attention. Snow, as a component of the cryosphere, has an important role in the water cycle and surface energy budget (Lemke et al., 2007; Vavrus, 2007), and it also strongly impacts socio-economic activities such as the tourism industry in some regions (Gonseth, 2013; Pons et al., 2012).

In the last years several studies have analyzed —using both observations and model simulations— the evolution of several indicators associated with snow: snow frequency, cover and extent, and length of the snow season, among others (Pons et al., 2010; Morán-Tejeda et al., 2013; Piazza et al., 2014, etc.). In general, these studies agree on a shortening of the snow season (Choi et al., 2010) and a decreasing snow cover extent (Lemke et al., 2007) in the Northern Hemisphere at the end of the 20th century (see García-Ruiz et al., 2011, and references therein) which also continues in the 21st century (Räisänen, 2008; Räisänen and Eklund, 2012). Other studies have analyzed the influence of temperature and precipitation on snow cover trends; for instance, Clark et al. (1999) studied Eurasian winter snow extent and found that in regions where the mean winter temperature was well below zero, snow extent was mainly controlled by precipitation. However, in the transient regions where the mean winter temperature was relatively close to zero, the temperature control was dominant. This changing influence of temperature or temperature-precipitation in snow in different regions has important implications for the analysis of future projections, since the climate change signal for temperature is more robust than for precipitation in existing climate change projections. Therefore, snow projections in regions mainly influenced by temperature may also have a more robust climate change signal.

In Europe, a statistically significant decrease has been detected in the Alps since the early 80s in the mean snow depth, the duration of snow cover and the number of snowfall days, with more pronounced trends in the medium and lower altitudes (Laternser and Schneebeli, 2003; Lemke et al., 2007). This decrease has been mainly attributed to an increase in mean temperature (Scherrer et al., 2004; Hantel and Hirtl-Wielke, 2007), mainly at lower elevations. A significant decreasing snow-pack trend has been also detected in the Pyrenees (López-Moreno, 2005; Morán-Tejeda et al., 2013), but attributed in this case to changes in both precipitation and temperature due to the medium and high altitudes. In a recent work, Buisan et al. (2015) studied the relationship between the number of snow days in the Pyrenees and other factors such as elevation, distance to the sea and weather types, finding a decreasing trend for the period 1971-2000.

A number of recent applications of Regional Climate Models (RCMs) with respect to European snow cover and snowfall scenarios have also been carried out in the last years. These two variables are related since snow cover changes can partly be explained by changes in snowfall amounts (as reflected by a change in the number of snow days), in addition to changes in the melt rate of an existing snow pack. Steger et al. (2012) found that the RCMs are capable of simulating the general spatial and seasonal variability of Alpine snow cover and found a shortening of the snow cover season in the twenty first century projections, with temperature changes appearing to be the dominant factor for the pronounced decrease

in all analyzed snow parameters throughout the twenty first century. Using high resolution RCM output, de Vries et al. (2014) showed that mean and extreme snowfall in most parts of western and central Europe are projected to reduce strongly in the future (2071-2100) while in a study for northern Europe (Räisänen, 2015), twelve regional model simulations of twenty-first century climate suggest a decrease in the winter total snowfall in nearly all of the area.

The objective of the present study is to analyze the historical and future projected regional snowfall trends in a broad area of Northern Spain —including the Cantabrian Range, the Central System and part of the Iberian System and the Pyrenees— building on a previous work by Pons et al. (2010) and focusing on annual snowfall occurrence (Number of Snowfall Days, NSD). These authors identified temperature as the main variable influencing the interannual variability of NSD in their dataset of medium to low altitude stations (with an interannual correlation of -0.72). Since the climate change signal for temperature is robust (as mentioned earlier in this introduction), this is an opportunity to explore future snowfall projections in this area. In particular, we explore the ability of an ensemble of regional climate models from the EU-funded ENSEMBLES project to properly reproduce the observed trends (both with "perfect" reanalysis boundary conditions and driven by the GCM outputs from the 20C3M historical scenario) and analyze the climate change signal produced in a future scenario (A1B) until the mid 21st century. We also analyze whether the observed relationship between temperature and NSD is preserved in the historical and future projections.

In the first part of the paper we present the different datasets considered in this work (Sec. 2). Secondly, we analyze the capability of the ERA40–driven RCM simulations to reproduce the climatology and trends observed for the snowfall frequency in the period 1961–2000 (Sec. 3). Then, we consider the GCM–driven simulations in order to analyze the trends projected by the RCMs under the historical (20C3M) and future (A1B, for the period 2011–2050) scenarios (Sec. 4). In section 5 we study the correlation with temperature and, finally, we synthesize the main results and conclusions of this work (Sec. 6).

2 Area of Study and Available Data

2.1 Observations

In this paper we consider 33 stations at medium to low heights (ranging from 60 to 1350 m) in Northern Iberia (see Fig. 1(a) and Table 1 for more details) which have been analyzed by Pons et al. (2010) in a previous study; the stations belong to the Spanish Meteorological State Agency (AEMET). Daily data for snowfall occurrence and mean temperature (obtained as the mean value of maximum and minimum temperatures) was available for the period 1961-2000. Snowfall occurrence is an indication of whether snowfall was reported in a 24-hour period, regardless of the amount (measurable snow on the ground is not even required to issue a report). The annual NSD inferred from this binary variable is then used throughout the study. By convention, the years considered in this paper don't correspond to natural years: they cover the period from September to May, preventing the winters to be artificially split into two separate years (summer months June, July and August —when practically no snowfall occurs— were excluded from this study).

The analysis of temperature is included in this work in order to explore the correlations with snowfall occurrence in present and future climates, following the results obtained in Pons et al. (2010) in which this variable showed the highest correlation. However, in order

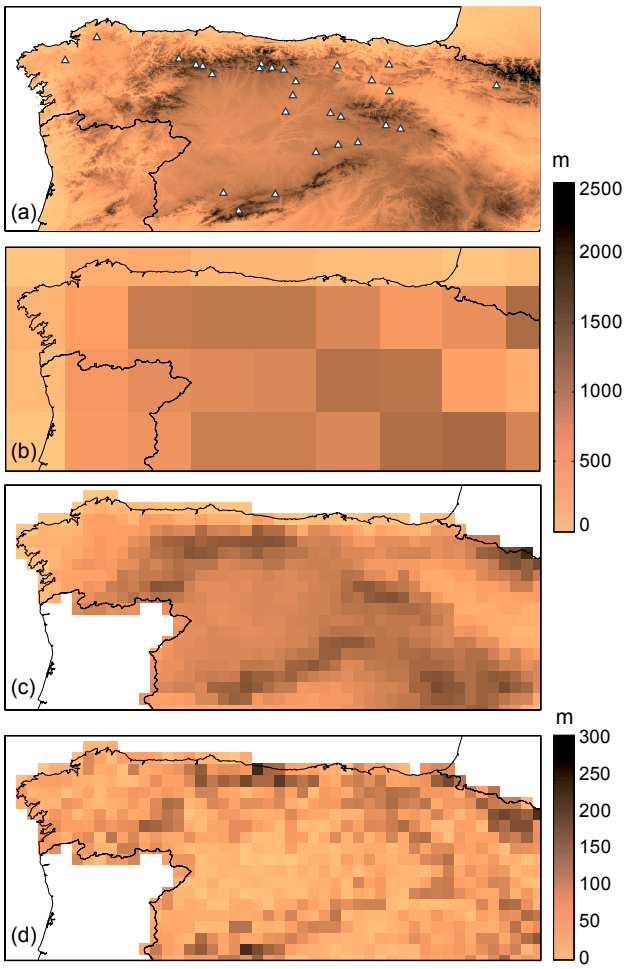

Fig. 1 (a) Orography of the Northern Iberian peninsula as given by GTOPO30 and spatial distribution of the stations used in the study (see Table 1 for geographical details). (b) ERA40 orography. (c) Mean and (d) standard deviation of the orography of the RCMs over the regular 25km grid.

to compare the observations with the RCM data, some stations will be discarded in this study (see sec. 2.3 for more details).

In the previous study by Pons et al. (2010) all the analysis was focused on the period 1975-2000, since the observed trend was found to be more significant for this shorter period than for the whole available period (1961-2000). In this study, however, the whole period has been considered to harmonize the length of the historical (1961-2000) and future (2011-2050) periods analysed. Moreover, the GCM-driven RCM runs have not been developed to reproduce the interannual variability observed in this period but the historical trend and, therefore, the analysis of a shorter period could lead to misleading results.

Station	Lat.	Lon.	Height	NSD	NSD_r	$Height_\mu$	$Height_\sigma$	$Height_d$
GRADO #*	43.38	-6.06	60	2.1	2.0	507	114.5	447
SANTESTEBAN #*	43.13	-1.66	131	4.8	4.8	579	104.4	448
VILLACARRIEDO #*	43.23	-3.80	212	4.8	4.8	719	82.8	507
MONTAOS-ORDES	43.04	-8.42	306	1.7	1.6	266	43.3	-40
AS PONTES DE GARCIA #	43.45	-7.86	343	4.0	3.8	522	62.1	179
CENICERO INDUSTRIAL #	42.48	-2.64	430	8.7	8.3	586	86.0	156
MIRANDA DE EBRO #	42.68	-2.96	520	9.8	9.2	598	62.1	78
URRUNAGA PRESA	42.96	-2.65	540	7.5	7.1	651	76.6	111
VILLARCAYO	42.94	-3.57	595	14.1	13.4	833	61.8	238
JAVIERREGAY	42.59	-0.74	690	8.9	8.7	915	145.4	225
MONZON DE CAMPOS #	42.12	-4.49	754	7.9	7.9	782	30.0	28
OSORNO	42.41	-4.36	809	10.0	9.6	775	54.9	-34
SAN MIGUEL DE BERNUY	41.40	-3.95	839	12.9	13.1	923	50.4	84
PANTANO DE STA. TERESA #	40.67	-5.60	840	13.1	12.7	911	27.6	71
ALAR DEL REY #	42.66	-4.31	851	17.6	17.1	921	53.9	70
SAN ESTEBAN DE GORMAZ #	41.57	-3.20	860	12.7	12.6	960	18.1	100
RETUERTA	42.03	-3.51	900	20.9	19.6	962	21.6	62
LINARES DEL ARROYO #	41.53	-3.56	911	14.0	13.6	936	60.9	25
BESCOS DE GARCIPOLLERA *	42.63	-0.50	920	14.8	14.1	1367	192.8	447
TORRECILLA DEL MONTE	42.09	-3.69	949	7.9	7.9	963	20.5	14
LA MAGDALENA #	42.78	-5.80	998	17.6	16.9	1088	118.0	90
PANTANO DE CERVERA	42.87	-4.53	1000	23.7	23.3	1129	115.1	129
GARRAY	41.82	-2.45	1010	9.8	9.7	1151	40.8	141
PANTANO DE REQUEJADA #*	42.91	-4.53	1024	26.8	26.4	1409	103.0	385
BOCA DE HUERGANO	42.97	-4.93	1104	36.5	35.0	1389	79.2	285
PRIORO #	42.89	-4.96	1123	35.9	35.7	1344	111.5	221
AVILA 'OBSERVATORIO'	40.65	-4.68	1130	17.5	16.7	1158	46.1	28
EMBALSE CUERDA DEL POZO	41.88	-2.70	1150	27.4	26.9	1197	138.4	47
RABANAL DE LUNA #	42.93	-5.97	1150	36.5	36.0	1394	50.7	244
GENESTOSO	43.06	-6.39	1180	50.5	50.0	1356	161.0	176
HUERGAS DE BABIA	42.96	-6.09	1222	46.6	46.4	1408	62.0	186
PANTANO DE CAMPORREDONDO #	42.90	-4.74	1253	39.6	39.2	1409	93.1	156
ZAPARDIEL DE LA RIBERA	40.36	-5.33	1353	27.7	27.9	1255	80.2	-98
Mean Values	42.42	-4.26	823	18.0	17.6	981	77.8	158

Table 1 Name, location (latitude and longitude, in degrees), height (m) and mean annual number of snow days (NSD) of all stations for the period 1961–2000. The last four columns correspond to the closest RCM grid points to each station for the nine RCMs and indicate the multi-RCM mean annual number of snow days (NSD_r) for the same period, the mean ($Height_\mu$) and the standard deviation ($Height_\sigma$) of the elevation, and its difference with the actual height of the station ($Height_d$). The stations in which this height difference was greater than 300 m are highlighted with an asterisk (*). Stations with temperature records are indicated with #.

2.2 Model simulations

The EU-funded project ENSEMBLES (http://www.ensembles-eu.org) was a collaborative effort of different European meteorological institutions focused on the generation of climate change scenarios over Europe, including a large variety of communities and state-of-the-art methodologies and techniques. In particular, dynamical downscaling was performed using different regional climate models (RCMs) run by different institutions (see the list in Table 2) over a common area covering the entire continental European region and with a common resolution of approx. 25 km, although with different native rotated grids for each model (the ICTP model is not considered in this study since it doesn't include the variable snow flux).

The RCMs were driven both by the ERA40–reanalysis of the European Centre for Medium Range Weather Forecasts (ECMWF, Uppala et al., 2005), for a common period

Table 2 Summary of the twelve RCMs from the ENSEMBLES project with snow data. The columns are the acronym used in the paper, the institution running the simulation, the model used and their corresponding references. The RCMs marked with an asterisk (*) were discarded in this study to avoid model redundancy (HRQ3 and HRQ16) or due to problems with the dataset (SMHI).

Acronym	Institution	Model	Reference
C4I	Comunity Climate Change Consortium for Ireland	RCA3	Samuelsson et al. (2011)
CNRM	Centre National de Recherches Meteorologiques	ALADIN-Climat	Radu et al. (2008)
DMI	Danish Meteorological Institute	HIRHAM	Christensen et al. (2006)
ETHZ	Swiss Federal Institute of Technology	CLM	Jaeger et al. (2008)
HRQ0	Hadley Center/UK MetOffice	HadRM3 Q0	Collins et al. (2006)
HRQ3(*)	Hadley Center/UK MetOffice	HadRM3 Q3	Collins et al. (2006)
HRQ16(*)	Hadley Center/UK MetOffice	HadRM3 Q16	Collins et al. (2006)
KNMI	Koninklijk Nederlands Meteorologisch Instituut	RACMO	van Meijgaard et al. (2008)
METNO	The Norwegian Meteorological Institute	HIRHAM	Haugen and Haakensatd (2005)
MPI	Max Planck Institute for Meteorology	M-REMO	Jacob et al. (2001)
SMHI(*)	Swedish Meteorological and Hydrological Institute	RCA	Kjellström et al. (2005)
UCLM	Universidad de Castilla la Mancha	PROMES	Sanchez et al. (2004)

Table 3 Matrix of the GCM–RCM coupling experiments from the ENSEMBLES project (van der Linden and Mitchell, 2009) used in this study. GCMs and RCMs are shown in columns and rows, respectively. G1: ARPEGE , G2: BCM, G3: ECHAM5-r3, G4: HadCM3-Q0, G5: HadCM3-Q16.

RCM\GCM	ERA40	G1	G2	G3	G4	G5
C4I	x					x
CNRM	x	x				
DMI	x	x	x	x		
ETHZ	x				x	
HRQ0	x				x	
KNMI	x			x		
METNO	x		x		x	
MPI	x			x		
UCLM	x				x	

of 40 years (1961–2000), and by different Global Circulation Models (GCMs) based on the 20C3M (1961–2000) and A1B (2001–2050) scenarios (Nakićenović, 2000; Nakićenović and Swart, 2000); in all cases, daily records of snow flux and temperature were downloaded from the DMI ENSEMBLES server (http://ensemblesrt3.dmi.dk/data; the data used correspond to the latest version available up to February 2015). The RCM simulations under both the 20C3M (historical) and A1B (future) scenarios were driven by one or several GCMs, as shown in Table 3.

A basic quality control of the RCM data revealed some problems in the SMHI dataset, exhibiting very small NSD values. Therefore, the SMHI model was not considered in this paper. Moreover, in order to avoid model duplicity, only the version with 'normal' climate sensitivity of the Hadley models (HRQ0) was included in the ensemble, discarding the version with 'low' (HRQ3) and 'high' (HRQ16) climate sensitivities (Collins et al., 2010).

Besides the RCM outputs we also analyze the global ERA40 reanalysis (Uppala et al., 2005), produced by the European Centre for Medium Range Weather Forecasts (ECMWF) in collaboration with many institutions. This reanalysis was obtained from the ECMWF's MARS server for the period September 1961 to August 2000 on its native resolution of 1.125° x 1.125°. An analysis of the GCM output itself was not possible as neither the CERA–database of the World Data Center for Climate (http://cera-www.dkrz.de/CERA/)

nor the DMI ENSEMBLES server (for the HadCM3-Q0 and HadCM3-Q16 models) provides snowfall data for these models.

2.3 Data Harmonization

In order to avoid the known drizzle effect of the climate models (Hay and Clark, 2003; Piani et al., 2010) which leads to an overestimation of the probability of rain and snowfall occurrence, snowfall frequency (NSD) was obtained from snow flux (kg m-2 s-1) using a threshold of 1 mm/day (1/86400 kg m-2 s-1). Moreover, for consistency with observations, mean temperature was obtained as the mean value of the maximum and minimum daily temperatures provided by the models.

Since each RCM has a different rotated grid, all of them were interpolated by nearest neighbours to a common 0.2° (approx. 20km) regular grid shown in Fig. 1. Fig. 1c-d shows the mean and standard deviation of the RCM elevations interpolated to this common grid. Note that the highest variability is obtained in regions with complex orography. In order to properly compare the stations and the RCM results, the height of each of the 33 stations was compared to the ensemble mean height of the closest RCM grid point (Column 7 in Table 1), discarding those stations differing by more than 300 m (highlighted with an asterisk in Table 1). This criterion was chosen since the maximum inter-model standard deviation of the orography in the study region is around 300 m and therefore the station elevation will be close to the grid cell orography of most RCMs. Hereinafter we will consider the resulting 28 stations. This implies that only 12 of the initial 16 stations with temperature records will be considered when analyzing the correlation between NSD and temperature.

3 ERA40–driven Simulations

In this part of the study we use the ERA40–driven RCM simulations in order to analyze the capability of the models to reproduce the NSD climatology, trend and interannual variability observed at the 28 stations (see Table 1 and Sec. 2.1 for more details).

Figure 2 shows the annual NSD climatologies for the period 1961–2000 given by the observations, ERA40 and the RCMs driven by ERA40. In general terms, all the RCM simulations exhibit a similar spatial pattern, with spatial correlations with observations ranging between 0.58 and 0.87 (see the last numbers in the titles of Fig. 2). The most noticeable difference is that simulations for C4I, CNRM and ETHZ (panels d, g, and k) underestimate snowfall. In order to explore this difference, a further analysis of all the RCMs orography and mean temperature fields was performed (not shown in this paper). The surface orography is realistically represented in all cases and these three models don't exhibit higher mean temperature fields than the rest; hence, snowfall underestimation is probably due to deficiencies in the parameterization of precipitation microphysics in these models.

In order to validate the performance of the RCMs we compare the observed and simulated trends and the interannual variability of the corresponding spatially averaged annual series. To this aim we consider the mean annual NSD value over the 28 stations (for the observations) and over the closest model gridboxes to the 28 stations (for the simulations). The first number in the title of each panel in Fig. 2 shows the trends of the corresponding series —significant trends at a 95% level are marked with an asterisk,— whereas the second number indicates the (inter-annual) correlation for the period 1961–2000.

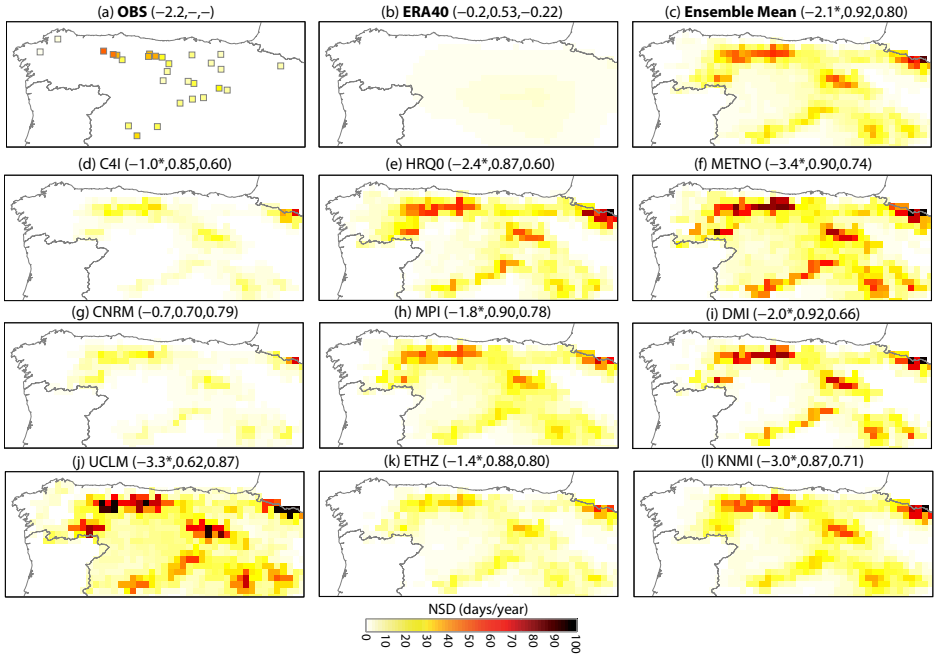

Fig. 2 Climatologies of NSD in the period 1961–2000 given by (a) the observations in the 28 stations (b) ERA40 and (d)–(l) the ERA40-driven simulations of the eleven RCMs used in this study (see Table 2) —the RCM ensemble mean results are shown in panel (c).—- The first number in the title of each panel shows the spatially averaged NSD trend in days/decade; trends significant at the 95% level are highlighted with an asterisk. The second number gives the temporal (interannual) correlation between the simulated and observed NSD time series, and the third number the corresponding spatial correlation. In all cases, only the 28 RCM gridboxes closest to the stations were considered in the analysis.

All the RCMs present negative trends —significant except the CNRM model,— ranging from −3.4 days/decade to −0.7 days/decade, with similar slopes than the observed ones, with the exception of the models which underestimate snowfall (panels d, g and k). Note that higher trends would be obtained for these models if they were bias-corrected (rescaled) to avoid underestimation; however we keep the original raw RCM values to assess to performance of the original ensemble, which will be subsequently used later in the paper to infer future trend projections driven by different GCMs. Moreover, all models exhibit high interannual correlation coefficients (over 0.85 with the exception of CNRM and UCLM), thus indicating a good performance in reproducing the temporal evolution of the NSD.

In order to appreciate more clearly its temporal evolution, Fig. 3 shows the interannual variability of the NSD averaged over the 28 stations/gridboxes in the period 1961–2000 for the ensemble of nine RCMs (indicated by the grey shadow, spanning from the minimum to the maximum value), together with the observations (red line), the ERA40 direct outputs (dashed black line), and the ensemble mean (black line). Fig. 3b shows the corresponding anomaly series, obtained after removing the mean of each of the models. Firstly, note that the observed NSD values are contained within the ensemble of RCMs. Secondly, note that the ensemble mean adequately reproduces the observed interannual variability —with a correlation of 0.92 in the period 1961-2000, as shown in Fig. 2c— and exhibits a very similar trend to the observations. Finally, ERA40 clearly underestimates the observed NSD

(Fig. 2b and Fig. 3) and is not able to reproduce the observed interannual variability (with a correlation coefficient of 0.53) nor the trend. The lower resolution of ERA40 and hence its lower orography (see Fig. 1b) is probably the main reason for its poor performance in representing the observed NSD values. This clearly shows the added value of the RCMs in this study, since they allow to properly reproduce the observed NSD climatology and trend when downscaling a reanalysis which simulates inadequately this variable.

Fig. 3 also displays the trend values for the period 1975-2000, clearly showing larger trends for the shorter period due to a small increase in the observed NSD between 1960 and 1970, which is reproduced by the ERA40-driven RCM simulations. However, all the analysis in this paper was performed using the 1961-2000 period for the reasons explained at the end of section 2.1.

A similar trend analysis was also performed for mean temperature obtaining a larger agreement among all RCMs (ranging from 0.1 to 0.2 °C/decade) and the observations (0.2 °C/decade), as shown in the first column of Table 4. In this case the temperature trend obtained directly from the ERA40 reanalysis series (0.4 °C/decade) was closer to the observations than the NSD trend.

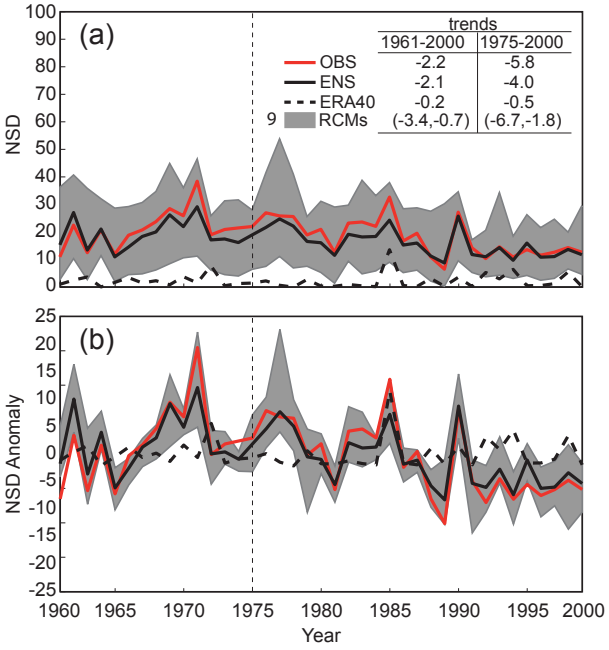

Fig. 3 (a) Annual NSD observations (red line) and RCM outputs from ERA40-driven simulations (grey shadow), averaged over the 28 stations/gridboxes. (b) Annual NSD anomalies obtained after removing the models' means. The solid and dashed black lines show the ensemble mean (ENS) and the direct ERA40 output, respectively. The number in the left of the RCM legend indicates the number of members forming the ensemble. The inset shows the trends (NSD/decade) over the 1961-2000 and 1975-2000 periods for the different models (the minimum and maximum values are shown for the RCM ensemble).

Table 4 Trends of NSD (days/decade) and temperature (°C/decade) during the period 1961–2000 for the RCMs nested to ERA40 and to the different GCMs in the 20C3M scenario —the last column shows the results for the multi-GCM ensemble.— The last row shows the multi-RCM ensemble mean (ENS) corresponding to each of the driving GCMs. Only the trends highlighted with an asterisk (*) are significant at a 95% level. Note that for the observations (ERA40 reanalysis) series, there is a trend of -2.2 (-0.2) days/decade for the NSD and 0.2* (0.4*) °C/decade for the temperature (not shown in the table).

RCM\GCM	ERA40	G1	G2	G3	G4	G5	Multi-GCM
C4I	(-1.0*, 0.2)					(-0.2, 0.1)	
CNRM	(-0.7 , 0.1)	(-0.6, 0.2*)					
DMI	(-2.0*, 0.2*)	(-0.4, 0.2*)	(-0.6, 0.0)	(-0.6, 0.1)			(-0.5, 0.1*)
ETHZ	(-1.4*, 0.1)				(-1.3, 0.3*)		
HRQ0	(-2.4*, 0.2*)				(-2.4*, 0.4*)		
KNMI	(-3.0*, 0.1)			(-0.4, 0.1)			
METNO	(-3.4*, 0.1)		(-1.2, 0.0)		(-2.4, 0.2*)		(-1.8, 0.1)
MPI	(-1.8*, 0.2)			(0.2, 0.1)			
UCLM	(-3.3*, 0.2*)				(-8.5*, 1.0*)		
ENS	(-2.1*, 0.2)	(-0.5, 0.2*)	(-0.9, 0.0)	(-0.3, 0.1)	(-3.6*, 0.5*)	(-0.2, 0.1)	(-1.5*, 0.2*)

4 GCM–driven Projections

Table 4 shows the trends corresponding to the ensemble of RCM–GCM couplings for the same period as in the previous section (1961-2000), considering the historical 20C3M runs. In some cases these trends are comparable to those obtained for the ERA40–driven simulations (the trends for the ERA40-driven simulations are also included in the table to facilitate the comparison) but the variability of the results is largely conditioned by the particular driving GCM, both for snowfall and temperature. The multi-model GCM-RCMs ensemble mean shows a good performance, with significant trends of -1.5 days/decade and 0.2 °C/decade, similar to the observed ones (-2.2 days/decade and 0.2 °C/decade).

Table 5 shows the corresponding trends for the future (2011–2050) projections corresponding to the A1B scenario runs. Note that most of the trends are significant in this period, ranging from -3.7 to -0.5 days/decade, indicating a significant decreasing trend for the NSD of -2.0 days/decade, according to the multimodel ensemble mean.

In order to graphically illustrate the influence of the driving GCM on the variability of the ensemble, Fig. 4a-c shows the composite series of the historical (20C3M) and future (A1B) anomalies (w.r.t. the 1961-2000 period) for the ensemble of all RCM–GCM simulations and those RCMs coupled to the HadCM3-Q0 global model and the ECHAM5-r3 global model separately (the two GCMs with the largest number of RCMs coupled to them, four and three, respectively). The models coupled to ECHAM5-r3 (panel c) show very little spread while those coupled to HadCM3-Q0 show a considerably greater spread in the A1B period (2001-2050). This change is due to a discontinuity caused by the changing scenario of the corresponding GCMs in year 2000 (from 20C3M to A1B), as shown in Figures Fig. 4d-f, where the corresponding anomaly series for the 2001-2050 have been re-centered (shifted to the ensemble mean). The resulting series show a similar interannual variability clearly ilustrating that the greatest uncertainty by far is associated with the particular GCM used.

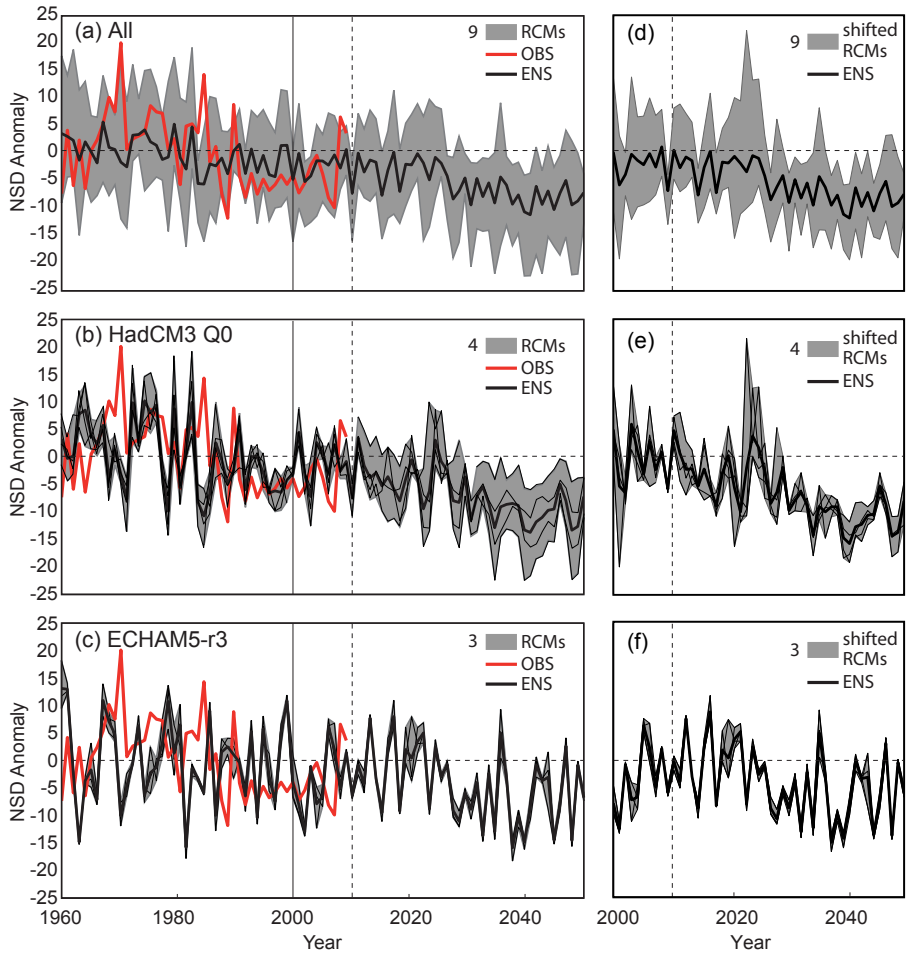

Fig. 4 Observations and historical (20C3M, 1961-2000) and future (A1B, 2001-2050) anomalies (w.r.t. the mean of the period 1961-2000) for the ensemble of all RCMs (a,d) and for the sub-ensembles driven by the HadCM3 Q0 (b,e) and ECHAM5-r3 (c,f). The mean of the anomalies of each of the RCMs in the period 2001-2050 has been shifted to the ensemble mean in panels (d-f) to avoid the shifts in the RCM simulations between the 20C3M and A1B periods. In all cases the red line represents the observations (OBS) and the black bold line represents the mean of the ensembles (ENS). In panels b-c and e-f the black thin lines represent each RCM–GCM simulation. The numbers in the legends indicate the number of members forming each ensemble.

5 Correlation with temperature

The relationship of NSD with annual rain frequency and mean temperature was analyzed by Pons et al. (2010), reporting correlation coefficients of 0.27 and -0.72, respectively, for the period 1957–2002. Taking into account this result, in the present paper we analyze only the correlation with mean temperature synthesizing the results in Table 6 (note that these results are based on only 12 stations with temperature records; see Table 1). This table shows the correlations considering the outputs of the RCMs nested with ERA40 and with

Table 5 Trends of NSD (days/decade) and temperature (°C/decade) during the period 2011–2050 for the RCMs nested to the different GCMs in the A1B scenario runs. Only the trends highlighted with an asterisk (*) are significant at a 95% level.

RCM\GCM	G1	G2	G3	G4	G5	Multi-GCM
C4I					(-0.5*, 0.4*)	
CNRM	(-1.2*, 0.4*)					
DMI	(-1.1*, 0.4*)	(-1.5, 0.2*)	(-2.6*, 0.3*)			(-1.9*, 0.3*)
ETHZ				(-1.5*, 0.6*)		
HRQ0				(-3.0*, 0.6*)		
KNMI			(-1.9, 0.3*)			
METNO		(-3.2*, 0.2*)		(-3.7*, 0.5*)		(-3.6*, 0.4*)
MPI			(-2.1, 0.3*)			
UCLM				(-2.3*, 0.4*)		
ENS	(-1.2*, 0.4*)	(-2.3*, 0.2*)	(-2.2*, 0.3*)	(-2.6*, 0.5*)	(-0.5*, 0.4*)	(-2.0*, 0.4*)

Table 6 Correlations between the NSD and temperature simulated for the RCMs nested with ERA40 (second column) and with the different GCMs considering both the 20C3M (first number in the parenthesis) and A1B (second number) scenarios for the periods 1961–2000 and 2011–2050, respectively. Note that the correlation in the first period between the observed (reanalysis) series was -0.63 (-0.32), not shown in the table.

RCM\GCM	ERA40	G1	G2	G3	G4	G5	Multi-GCM
C4I	-0.61					(-0.24, -0.42)	
CNRM	-0.40	(-0.29, -0.69)					
DMI	-0.70	(-0.67, -0.75)	(-0.68, -0.78)	(-0.66, -0.77)			(-0.59,-0.81)
ETHZ	-0.56				(-0.76, -0.67)		
HRQ0	-0.73				(-0.80, -0.82)		
KNMI	-0.62			(-0.34, -0.65)			
METNO	-0.60		(-0.61, -0.79)		(-0.85, -0.80)		(-0.81,-0.88)
MPI	-0.65			(-0.46, -0.67)			
UCLM	-0.20				(-0.92, -0.76)		
ENS	-0.61	(-0.51, -0.76)	(-0.66, -0.80)	(-0.50, -0.71)	(-0.90, -0.84)	(-0.24, -0.42)	(-0.76,-0.89)

the different GCMs under both the 20C3M and A1B scenarios, for the periods 1961–2000 and 2011–2050, respectively.

Excluding CNRM and UCLM, all the RCMs forced with reanalysis data are able to reproduce reasonably well the observed dependence between the NSD and temperature in the period 1961–2000, with correlation values ranging from -0.73 to -0.56. Moreover, when comparing the results corresponding to the historical runs (20C3M) and the future scenarios (A1B) we found that the correlation is larger for the latter in most of the cases which may be related to the higher trends simulated by the regional models under the A1B scenario.

6 Conclusions

In this paper we have analyzed the performance of the ERA40– and GCM–driven RCM simulations to reproduce the spatial pattern and the interannual variability of the number of snowfall days in 28 stations of northern Spain, following the study by Pons et al. (2010).

One of the most clear conclusions of this work is that ERA40 cannot be used on its own in NSD trend assessment studies, although it properly reproduces the trend of temper-

ature (the most important variable influencing snowfall in this region). Its low resolution is the most likely reason for not being able to represent either the interannual variability or the observed trend. However, practically all the RCM ERA40–driven simulations analyzed in this study capture properly the NSD spatial pattern (correlations ranging between 0.58 and 0.87), the interannual variability (correlations between 0.62 and 0.92), as well as the observed trends of the last quarter of the 20th century (trends ranging from -3.4 to -0.7 days/decade). Some of the models (C4I, CNRM and ETHZ) exhibited an underestimation of the climatological NSD yielding smaller trend values.

In the case of the GCM–driven simulations in the historical period (20C3M) the RCM results are quite variable with trends ranging from -8.5 to 0.2 days/decade although they practically all capture the sign and, mainly in the case of the HadCM3-Q0, the intensity of the NSD trends of the corresponding ERA40–driven simulation. Furthermore, the multi-model ensemble mean shows a good performance, with significant trends of -1.5 days/decade and 0.2 °C/decade, similar to the observed ones (-2.2 days/decade and 0.2 °C/decade). The trends for the future GCM–driven projections (A1B scenario, 2011–2050) are more consistent and significant than the historical ones, ranging in this case from -3.7 to -0.5 days/decade; the multi-model ensemble mean indicates future significant trends of -2.0 days/decade and 0.38 °C/decade, (33% and almost 50% higher than the ones simulated for the 1961-2000 period, respectively).

The correlation between the observed NSD and the temperature in the period 1961-2000 (-0.63) is preserved by both ERA40– and 20C3M scenario GCM–driven simulations (-0.61, -0.76, respectively). This relation between both variables is stronger in the future A1B projections (-0.89), leading to opposite significant trends for both variables in the future.

Finally, another interesting result from this study is the fact that the greatest uncertainty by far in the GCM-RCM simulations is due to the particular GCM used. This is in agreement with previous results found by Déqué et al. (2012), who found that the largest source of uncertainty for temperature and precipitation in the ENSEMBLES dataset came from the GCM (with the exception of Summer for precipitation). Although no proper separation of variance analysis has been performed in this paper, the results shown in Tables 4 and 5 and Fig. 4 clearly indicate that the fraction of variance explained by the GCM is very large in this case. Therefore, special care should be taken when constructing the multi GCM-RCM matrices in ensemble experiments for regional climate change in order to properly balance the contribution of each of the GCMs.

Acknowledgments

This research has received funding from the European Union's Seventh Framework Programme under grant agreements 606799 (INTACT Project). The RCM simulations used in this study were obtained from the European Union-funded FP6 Integrated Project ENSEMBLES (Contract number 505539). The authors are grateful to the Spanish Meteorological State Agency (AEMET) for providing us with partial support and the necessary data for this work, and to two anonymous reviewers, who provided insightful comments that greatly improved the original manuscript.

7 Compliance with Ethical Standards

To ensure objectivity and transparency in research and to ensure that accepted principles of ethical and professional conduct have been followed, authors should include information regarding sources of funding, potential conflicts of interest (financial or non-financial), informed consent if the research involved human participants, and a statement on welfare of animals if the research involved animals. Authors should include the following statements (if applicable) in a separate section entitled Compliance with Ethical Standards before the References when submitting a paper:

- **Disclosure of potential conflicts of interest:** the work complies with the Ethical Rules applied by this journal and has not been submitted (or published previously) to other journal. All the authors included have contributed to this work, both in the development and in the interpretation of the scientific results.
- **Research involving Human Participants and/or Animals:** not applicable in this case
- **Informed consent:** all the authos have consented the submission of this work and are prepared to collect documentation of compliance with ethical standards and send if it is requested during peer review or after publication.

References

Buisan, S. T., M. A. Saz, and J. I. López-Moreno, 2015: Spatial and temporal variability of winter snow and precipitation days in the western and central spanish pyrenees. *International Journal of Climatology*, **35**, 259–274, doi:10.1002/joc.3978.

Choi, G., D. A. Robinson, and S. Kang, 2010: Changing northern hemisphere snow seasons. *Journal of Climate*, **23**, 5305–5310, doi:10.1175/2010JCLI3644.1.

Christensen, O. B., M. Drews, J. H. Christensen, K. Dethloff, K. Ketelsen, I. Hebestadt, and A. Rinke, 2006: The HIRHAM Regional Climate Model Version 5 (β). Technical Report 06-17, DMI. Available at `http://www.dmi.dk/dmi/en/print/tr06-17.pdf`.

Clark, M. P., M. C. Serreze, and D. Robinson, 1999: Atmospheric controls on eurasian snow extent. *International Journal of Climatology*, **19**, 27–40.

Collins, M., B. B. B. Booth, B. Bhaskaran, G. R. Harris, J. M. Murphy, D. M. H. Sexton, and M. J. Webb, 2010: Climate model errors, feedbacks and forcings: a comparison of perturbed physics and multi-model ensembles. *Climate Dynamics*, **36 (9-10)**, 1737–1766, doi:10.1007/s00382-010-0808-0, URL `http://link.springer.com/article/10.1007/s00382-010-0808-0`.

Collins, M., B. B. B. Booth, G. R. Harris, J. M. Murphy, D. M. H. Sexton, and M. J. Webb, 2006: Towards quantifying uncertainty in transient climate change. *Climate Dynamics*, **27 (2)**, 127–147.

de Vries, H., G. Lenderink, and E. van Meijgaard, 2014: Future snowfall in western and central europe projected with a high-resolution regional climate model ensemble. *Geophysical Research Letters*, **41 (12)**, 4294–4299, doi:10.1002/2014GL059724, URL `http://dx.doi.org/10.1002/2014GL059724`.

Déqué, M., S. Somot, E. Sanchez-Gomez, C. M. Goodess, D. Jacob, G. Lenderink, and O. B. Christensen, 2012: The spread amongst ENSEMBLES regional scenarios: regional climate models, driving general circulation models and interannual variability. *Climate Dynamics*, **38 (5-6)**, doi:10.1007/s00382-011-1053-x, URL `http://link.springer.com/article/10.1007/s00382-011-1053-x`.

García-Ruiz, J. M., J. I. López-Moreno, S. M. Vicente-Serrano, T. LasantaMartínez, and S. Beguería, 2011: Mediterranean water resources in a global change scenario. *Earth-Science Reviews*, **105**, 121–139, doi:10.1016/j.earscirev.2011.01.006.

Gonseth, C., 2013: Impact of snow variability on the swiss winter tourism sector: implications in an era of climate change. *Climatic Change*, **119**, 307–320, doi:10.1007/s10584-013-0718-3.

Hantel, M. and L. M. Hirtl-Wielke, 2007: Sensitivity of alpine snow cover to european temperature. *International Journal of Climatology*, **27**, 1265–1275.

Haugen, J. E. and H. Haakensatd, 2005: Validation of HIRHAM version 2 with 50km and 25km resolution. General Technical report 9, RegClim, 159–173 pp. Available at `http://regclim.met.no/results/gtr9.pdf`.

Hay, L. E. and P. Clark, 2003: Use of statistically and dynamically downscaled atmospheric model output for hydrologic simulations in three mountainous basins in the western united states. *J. Hydrol.*, **282**, 56–75.

Jacob, D., et al., 2001: A comprehensive model inter-comparison study investigating the water budget during the BALTEX-PIDCAP period. *Meteorology and Atmospheric Physics*, **77 (1)**, 19–43.

Jaeger, E. B., I. Anders, D. Luthi, B. Rockel, C. Schar, and S. Seneviratne, 2008: Analysis of ERA40-driven CLM simulations for Europe. *Meteorologische Zeitschrift*, **17 (4)**, 349–367.

Kjellström, E., et al., 2005: A 140-year simulation of European climate with the new version of the Rossby Centre regional atmospheric climate model (RCA3). Reports Meteorology and Climatology 108, SMHI, 54 pp.

Laternser, M. and M. Schneebeli, 2003: Long-term snow climate trends of the swiss alps (1931-99). *International Journal of Climatology*, **23**, 733–750.

Lemke, P., et al., 2007: Observations: Changes in snow, ice and frozen ground. Technical Report –, Cambridge University Press, Cambridge, United Kingdom and New York, NY, USA. In: Climate Change 2007: The Physical Science Basis. Contribution of Working Group I to the Fourth Assessment Report of the Intergovernmental Panel on Climate Change.

López-Moreno, J. I., 2005: Recent variations of snow pack depth in the central spanish pyrenees. *Artic, Antartic and Alpine Research*, **37**, –.

Morán-Tejeda, E., S. Herrera, J. I. López-Moreno, J. Revuelto, A. Lehmann, and M. Beniston, 2013: Evolution and frequency (1970-2007) of combined temperature-precipitation modes in the spanish mountains and sensitivity of snow cover. *Regional Environmental Change*, **13(4)**, 873–885, doi:10.1007/s10113-012-0380-8.

Nakićenović, N., 2000: Greenhouse Gas Emissions Scenarios. *Technological Forecasting and Social Change*, **65**, 149–166, doi:10.1016/S0040-1625(00)00094-9.

Nakićenović, N. and R. Swart, 2000: Special report on emissions scenarios. Technical report, Intergovernmental Panel on Climate Change, Intergovernmental Panel on Climate Change, University Press, Cambridge, UK.

Piani, C., J. O. Haerter, and E. Coppola, 2010: Statistical bias correction for daily precipitation in regional climate models over europe. *Theor. Appl. Climatol.*, **99 (1–2)**, 187–192.

Piazza, M., J. Boé, L. Terray, C. Pagé, E. Sanchez-Gomez, and M. Déqué, 2014: Projected 21st century snowfall changes over the french alps and related uncertainties. *Climatic Change*, **122**, 583–594, doi:10.1007/s10584-013-1017-8.

Pons, M., A. Johnson, M. Rosas-Casals, B. Sureda, and E. Jover, 2012: Modeling climate change effects on winter ski tourism in andorra. *Climate Research*, **54(3)**, 197–207, doi:10.3354/cr01117.

Pons, M. R., D. San-Martín, S. Herrera, and J. M. Gutiérrez, 2010: Snow trends in Northern Spain: analysis and simulation with statistical downscaling methods. *International Journal of Climatology*, **30(12)**, 1795–1806, doi:10.1002/joc.2016.

Radu, R., M. Déqué, and S. Somot, 2008: Spectral nudging in a spectral regional climate model. *Tellus A*, **60 (5)**, 898–910.

Räisänen, J., 2008: Warmer climate: less or more snow? *Climate Dynamics*, **30**, 307–319, doi:10.1007/s00382-007-0289-y.

Räisänen, J., 2015: Twenty-first century changes in snowfall climate in northern europe in ensembles regional climate models. *Climate Dynamics*, doi:10.1007/s00382-015-2587-0.

Räisänen, J. and J. Eklund, 2012: 21st century changes in snow climate in northern europe: a high-resolution view from ensembles regional climate models. *Climate Dynamics*, **38**, 2575–2591, doi:10.1007/s00382-011-1076-3.

Samuelsson, P., et al., 2011: The rossby centre regional climate model rca3: model description and performance. *Tellus A*, **63**, 4–23, doi:10.1111/j.1600-0870.2010.00478.x.

Sanchez, E., C. Gallardo, M. A. Gaertner, A. Arribas, and M. Castro, 2004: Future climate extreme events in the Mediterranean simulated by a regional climate model: a first approach. *Global and Planetary Change*, **44 (1-4)**, 163–180.

Scherrer, S., C. Appenzeller, and M. Laternser, 2004: Trends in swiss alpine snow days: The role of local- and large-scale climate variability. *Geophysical Research Letters*, **31**, L13 215, doi:10.1029/2004GL020255.

437 Steger, C., S. Kotlarski, T. Jones, and C. Schär, 2012: Alpine snow cover in a changing
438 climate: a regional climate model perspective. *Climate Dynamics*, **41**, 735–754, doi:
439 10.1007/s00382-012-1545-3.
440 Trenberth, K. E., et al., 2007: Observations: Surface and atmospheric climate change. Tech-
441 nical Report –, Cambridge University Press, Cambridge, United Kingdom and New York,
442 NY, USA. In: Climate Change 2007: The Physical Science Basis. Contribution of Work-
443 ing Group I to the Fourth Assessment Report of the Intergovernmental Panel on Climate
444 Change.
445 Uppala, S., et al., 2005: The ERA-40 re-analysis. *Quarterly Journal of the Royal Meteoro-*
446 *logical Society*, **131 (612, Part B)**, 2961–3012, doi:10.1256/qj.04.176.
447 van der Linden, P. and J. Mitchell, (Eds.) , 2009: *ENSEMBLES: Climate Change and its*
448 *Impacts: Summary of research and results from the ENSEMBLES project*. Met Office
449 Hadley Centre, FitzRoy Road, Exeter EX1 3PB, UK, 160pp pp.
450 van Meijgaard, E., L. van Ulft, W. van de Berg, F. Bosveld, B. van den Hurk,
451 G. Lenderink, and A. Siebesma, 2008: The KNMI regional atmospheric climate
452 model RACMO, version 2.1. Technical report 302, KNMI, 43 pp. Available at
453 `http://www.knmi.nl/bibliotheek/knmipubTR/TR302.pdf`.
454 Vavrus, S., 2007: The role of terrestrial snow cover in the climate system. *Climate Dynamics*,
455 **29**, 73–88, doi:10.1007/s00382-007-0226-0.